Polarization-Based Sensing in Mesh Optical Networks for Early Earthquake Detection

Hasan Awad[1*], Fehmida Usmani[1, 2], Emanuele Virgillito[1], Rudi Bratovich[3], Stefano Straullu[4], Francesco Aquilino[4], Roberto Proietti[1], Rosanna Pastorelli[3] and Vittorio Curri[1]

(1) Politecnico di Torino, Italy, hasan.awad@polito.it
(2) National University of Sciences & Technology (NUST), Islamabad, Pakistan,
(3) SM-Optics, Italy
(4) LINKS Foundation, Italy

Abstract *We demonstrate interconnected meshed optical networks as sensing-localization grid for earthquake early detection. We integrate ground displacement data from seven local earthquakes, magnitudes four to six, into a Waveplate model to enhance a machine-learning algorithm that accurately detects primary waves and improves nearby urban safety.*

Introduction

Earthquakes often precede variations in strain rates at which the Earth's crust either stretches or compresses[1]. These changes, primarily induced by the arrival of primary waves, tens of seconds before the destructive surface waves struck, serve as significant indicators for upcoming seismic events[2]. Buried underground, optical fibers experience alteration in both mechanical and optical properties. This phenomenon broadens the potential for utilizing optical networks as distributed sensor networks for earthquake early detection[3]. Therefore, we have witnessed a recent emergence of Distributed Fiber Optic Sensors. These sensors leverage natural scattering processes, such as Distributed Acoustic Sensing (DAS) and Interferometric techniques[4]–[8]. Unlike DAS and interferometric techniques, our polarization sensing-based approach[9] requires no dedicated dark fibers or adding expensive equipment to the network, such as ultra-stable low-phase noise lasers. State-of-Polarization (SOP) based techniques monitor polarization changes of the modulated light propagating through traffic-carrying optical fibers[10]–[12]. These changes could be induced by anthropic activities[13],[14], or environmental events, such as earthquakes[15],[16]. In[9], we utilize a single sensing fiber within a terrestrial optical network. Using SYNGINE[17], we generate synthetically ground displacement data for a 4.9 magnitude earthquake, which are then converted into strain matrices by leveraging the Waveplate model. Subsequently, we employ a Bi-GRU based Machine Learning (ML) algorithm to detect primary wave arrival with a 97% accuracy rate and one-second ML detection time. In this manuscript, we extend the use of our polarization sensing approach, focusing on interconnected terrestrial optical mesh networks as a sensing and localization grid in the Modena region in Italy, and utilizing 7 real, instead of synthetic, earthquakes' displacement data, with magnitude values ranging from 4 to 6, to refine the ML model for a more generalized case scenario. In Section II, we detail SOP data extraction by the Waveplate model. Section III introduces the ML Model Validation, followed by Section IV and V, where we demonstrate Network implementation and Waveplate/ML/Localization results, respectively. Lastly, Section VI concludes the discussion.

SOP Data Extraction Methodology

A long optical fiber cable is, to a good approximation, equivalent to a concatenation of small sections, referred to as plates. The importance of segmenting the fiber into these sections is to define the effect of internal birefringence, stemming from fiber's construction imperfections, on the change of light's SOP. This is because, in a fiber section small enough, the internal birefringence can be considered uniform. Consequently, any deviation observed in SOP diverging from the anticipated uniform internal behavior effect indicates an external stressor. This approach is known as the Waveplate model[18]. We extend the use of this model to integrate the conventional i-DAS conversion in order to convert earthquake displacement values to strain-time matrices, where each 116 nm of displacement is equivalent to 11.6 nano-strain[19]. Multiple SOP evolution could be extracted from each Waveplate simulation for each earthquake strain values due to the fact that in each simulation the plates are inherently assigned to random orientations. A large set of SOP evolution data induced by each earthquake strain values is collected, from which we calculate the State of Polarization Angular Speed (SOPAS) for each SOP file[20]. The resulting SOPAS data is then utilized to train an ML algorithm capable of detecting primary wave's arrival for each seismic event, all ranging from magnitude 4 to 6. The trained ML algorithm will then be tested on an earthquake among the same range of magnitudes, highlighting the use of the whole smart sensing grid optical network. We chose SOPAS over SOP to minimize computational time, as SOP involves three parameters (S1, S2, and S3), while SOPAS requires only one.

ML Model Validation

Through the Italian National Institute of Geophysics and Volcanology (INGV)[21], we extracted displacement data for 7 local earthquakes that occurred in the Modena region. The earthquakes magnitudes chosen were M4, M4.3, M4.5, M4.7, M5.1, M5.3 and M5.8. The objective is to couple strain values induced by these displacements into fiber cables simulated with the aforementioned Waveplate model. A Temporal Fusion Attention Network (TFAN) is utilized for the ML training, in which we combined a Temporal Convolution Network[22], Long Short - Term Memory (LSTM) layers[23], and an attention mechanism. Almost 60% of the SOPAS data used for training, 20% for validation and 20% for testing. Exploiting the Waveplate model, we ran 50 simulations with different plates' orientations for each earthquake. Fig. 1 shows the model training and validation accuracy.

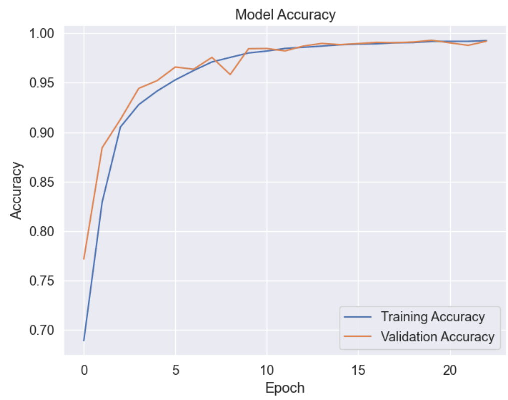

Fig. 1: ML Model Training and Validation Accuracy

The graph displays the accuracy of the ML model over a sequence of epochs. The model's training accuracy shown in blue increases rapidly, indicating effective initial training. The validation accuracy shown in orange evaluates the model's ability to predict new unseen data. The proximity of the two curves indicates that the model has been generalized well with a minimal risk of overfitting. As the number of epochs increases, both curves reach noticeable accuracy rates, implying that additional training is unlikely to yield significant improvements. The model showed a promising level of predictive precision for both training and validation datasets exceeding 95% of accuracy rates.

Seismic Fiber Network Implementation

For testing the model, we used the M4.3 earthquake in the region. The objective is to exploit an interconnection of optical fiber networks buried underground in nearby municipalities covering an area of less than 100 km^2, and use fibers from the mesh networks positioned at the exact geographical coordinates as the seismic stations for sensing and epicenter localization purposes. For sensing, we extracted the displacement data from three seismic stations (OPPE, MNTV and ZCCA) located in three distinct municipalities around the epicenter as shown in Fig. 2.

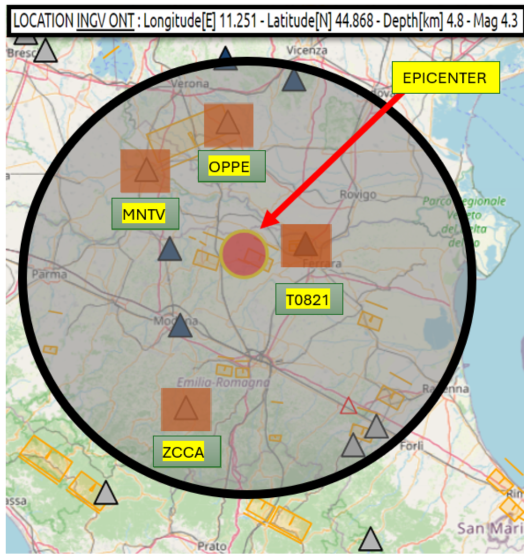

Fig. 2: M4.3 Earthquake Origin Time: 2012-05-23 21:41:18 (UTC) | Region: MODENA

A fiber substituting T0821 is used to localize earthquake's epicenter. The Optical Network Controller (ONC) overseeing all interconnected networks, will confirm primary wave arrivals from three sensing fibers/nodes as shown in Fig. 3, localize the epicenter by triangulating T0821, MNTV and ZCCA substitutes, and generate early warnings accordingly. Given the proximity of the three sensing seismic stations/corresponding fibers to the epicenter, the seismic wave reaches all stations almost at the same time. Consequently, this simultaneity does not impact significantly on the time available for the ONC to confirm the event and generate early warnings after the third confirmation.

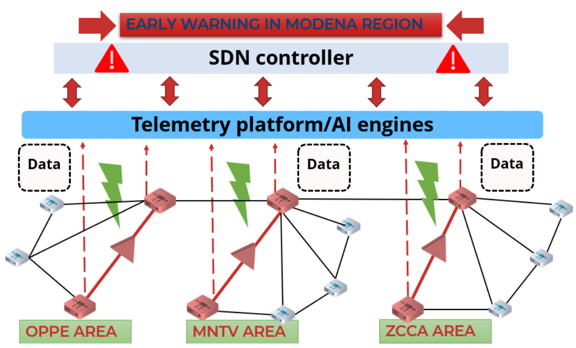

Fig. 3: Interconnected Sensing Grid in the Modena Region

Waveplate/ML Models and Localization Results

According to the Central Italian Appennines Velocity Model (CIA)[24], the time window between the primary wave and the arrival of surface wave at a seismic station increases with the increase of the station's distance from the earthquake's epicenter. As shown in Fig. 2, and according to INGV[21], MNTV and OPPE have almost the same distance from the epicenter (47.9 km and 49.3 km). Thus, Fig. 4 shows the average fiber strain substituting MNTV and ZCCA, where ZCCA is 61.4 km far from the epicenter.

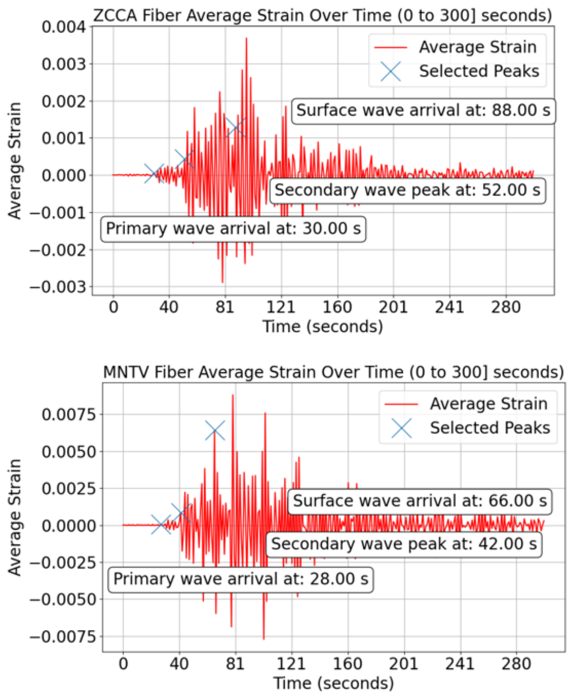

Fig. 4: Average Strain for ZCCA and MNTV Fiber Substitutes

The data were sampled over 300 seconds duration. The strain showed that MNTV fiber experienced a 24-seconds time lag between the primary wave and surface wave arrival (66-42), while the ZCCA fiber had a 36-seconds window (88-52).

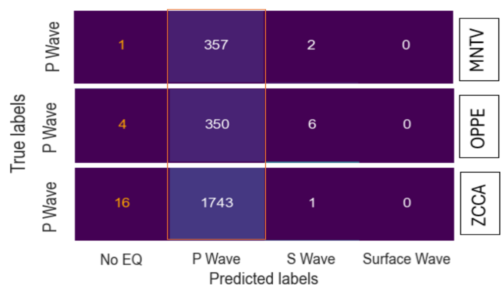

Fig. 5: Confusion Matrix for Three Stations/Fibers

ML results showed around 98% of accurate detection for primary waves according to confusion matrices for each station/fiber, as reported in Fig. 5, which shows the correct and wrong detection of the ML model for three stations/fibers. For instance, for ZCCA fiber, 16 wrong detected as "no earthquake" instead of being detected as primary wave (3rd row, 1st column), one wrong detection as secondary wave and zero as surface wave. The total correct detection for ZCCA fiber is 1743 out of 1760 primary waves. The same concept applies to other fibers substituting other seismic stations.

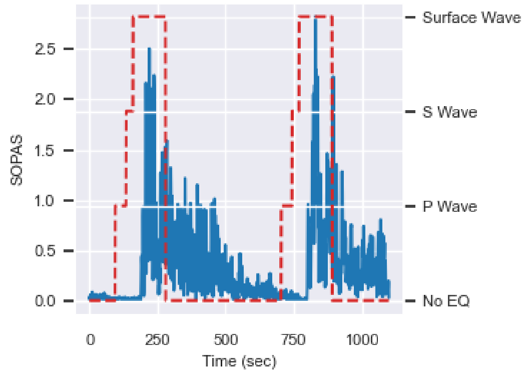

Fig. 6: Time needed for ML Detection for MNTV Fiber

The ML model took the same time to detect primary waves in all fibers substitutes. Fig. 6 shows one second ML detection time on the MNTV fiber and similarly for other fibers.

	Epicenter Location		Station to Epicenter Distance (km)		
INGV Recording	Longitude	Latitude	MNTV	ZCCA	T0821
	11.251	44.868	47.88	61.45	23.14
Triangulation Simulator	11.2846	44.8705	49.59	63.08	20.48

Tab. 1: INGV Recording and Triangulation Simulator

While Tab.1 shows the triangulation results applied by the ONC, which is used to localize the epicenter and prioritize early warning to municipalities close to the epicenter location and progress to those further away. This is done by forming a triangle around the epicenter leveraging the arrival time of the primary wave and precise coordinates of each node. T0821 shown in Fig. 2, a station around 20 km far from the epicenter, a key node to form the triangular shape. Consequently, the municipality where T0821 is located will be the first to be notified by the ONC for the upcoming seismic event, as there are only 16 seconds between the primary and surface wave arrival according to our simulation and to INGV recording. Accounting to the one-second ML detection time, urban areas within 20 km from the epicenter will have 15 seconds time window to implement earthquake countermeasures, while municipalities, where MNTV/OPPE and ZCCA are located, will have 23 and 35 seconds, respectively, according to what we mentioned earlier.

Conclusion

We investigated the use of interconnected fiber optic mesh networks as a sensing and localization grid for accurate ML-based earthquake early warning approach. Data were extrapolated from real earthquakes of different magnitudes recorded by INGV in the region of Modena, Italy.

Acknowledgements

The presented work has been supported by the Italian National Recovery and Resilience Plan (NRRP) of NextGenerationEU, a partnership on "Telecommunications of the Future" (PE00000001 - program "RESTART") and by the project FAAS funded by OpenFiber.

References

[1] T. Jordan, Y. Chen, P. Gasparini, *et al.*, *Operational Earthquake Forecasting: State of Knowledge and Guidelines for Utilization*. Rome, Italy: Istituto Nazionale di Geofisica e Vulcanologia, 2011. DOI: 10.4401/ag-5350.

[2] O. Kulhánek, *Seismic Waves In Anatomy of Seismograms*. Amsterdam, Netherlands: Elsevier Science, 1990. DOI: 10.1193/1.1585692.

[3] M. Mazur, N. Parkin, R. Ryf, *et al.*, "Continuous fiber sensing over field-deployed metro link using real-time coherent transceiver and das", in *Proceedings of European Conference on Optical Communication (ECOC)*, Basel, Switzerland, 2022, Mo4A.2.

[4] B. Dong, A. Popescu, V. Tribaldos, S. Byna, J. Ajo-Franklin, and K. Wu, "Real-time and post-hoc compression for data from distributed acoustic sensing", *Elsevier Science*, vol. 166, no. 105181, pp. 1–22, 2022. DOI: 10.1016/j.cageo.2022.105181.

[5] P. Jousset, T. Reinsch, T. Ryberg, *et al.*, "Dynamic strain determination using fibre-optic cables allows imaging of seismological and structural features", *Nature communications*, vol. 9, no. 2509, pp. 1–11, 2018. DOI: 10.1038/s41467-018-04860-y.

[6] G. Marra, D. M. Fairweather, V. Kamalov, *et al.*, "Transforming subsea optical cables into a giant network of environmental sensors", in *Proceedings of Optical Fiber Communication Conference (OFC)*, San Diego California United States, 2023, p. M2C.1. DOI: 10.1364/OFC.2023.M2C.1.

[7] G. Marra, C. Clivati, R. Luckett, *et al.*, "Ultrastable laser interferometry for earthquake detection with terrestrial and submarine cables", *Science*, vol. 361, no. 6401, pp. 486–490, 2018. DOI: 10.1126/science.aat4458.

[8] M. A. Soto and J. A. Ramírez, "Earthquake monitoring using fibre-optic distributed acoustic sensing", in *Proceedings of European Conference on Optical Communications (ECOC)*, Glasgow, United Kingdom, 2023, pp. 1441–1444. DOI: 10.1049/icp.2023.2585.

[9] F. Usmani, H. Awad, E. Virgillito, *et al.*, "Earthquake early warning through terrestrial optical networks: A bi-gru attention model approach on sop data", in *Proceedings of Optical Fiber Communications Conference (OFC)*, San Diego, California, United States, 2024, Tu3J.2.

[10] M. Cantono, J. Castellanos, S. Batthacharya, *et al.*, "Optical network sensing: Opportunities and challenges", in *Proceedings of Optical Fiber Communications Conference (OFC)*, San Diego, California, United States, 2022, M2F.1. DOI: 10.1364/ofc.2022.m2f.1.

[11] C. Carver and X. Zhou, "Polarization sensing over terrestrial optical fiber networks", *preprint Under Review at Nature Portfolio*, no. 1, pp. 1–17, 2024. DOI: 10.21203/rs.3.rs-3838279/v1.

[12] R. Bratovich, F. M. R., S. Straullu, *et al.*, "Surveillance of metropolitan anthropic activities by wdm 10g optical data channels", in *Proceedings of European Conference on Optical Communication (ECOC)*, Basel, Switzerland, 2022, Tu3B.6.

[13] H. Awad, E. Virgillito, S. Straullu, *et al.*, "Environmental sensing and localization via sop monitoring of im-dd optical data channels", in *Proceedings of OPTICA Sensing Congress (OSA)*, Munich, Germany, 2023, JTu4A.8. DOI: 10.1364/AIS.2023.JTu4A.8.

[14] E. Virgillito, S. Straullu, F. Aquilino, *et al.*, "Detection and localization of metropolitan anthropic activities by sop monitoring of im-dd optical data channels", in *Proceedings of International Conference on Photonics in Switching and Computing (PSC)*, Mantova, Italy, 2023, pp. 1–3. DOI: 10.1109/PSC57974.2023.10297183.

[15] H. Awad, F. Usmani, E. Virgillito, *et al.*, "Seismic detection through state-of-polarization analysis in optical fiber networks", in *Proceedings of SPIE Photonics West*, San Fransisco, California United States, 2024, pp. 12 835–48. DOI: 10.1117/12.3007808.

[16] E. Virgillito, S. Straullu, F. Aquilino, *et al.*, "Detection, localization and emulation of environmental activities using sop monitoring of imdd optical data channels", in *Proceedings of International Conference on Transparent Optical Networks (ICTON)*, Bucharest, Romania, 2023, Mo.D1.3. DOI: 10.1109/ICTON59386.2023.10207513.

[17] Incorporated Research Institutions for Seismology (IRIS). "Syngine: A Community-Driven Software Platform for Seismological Data Science". (2023), [Online]. Available: https://ds.iris.edu/ds/products/syngine/ (visited on 02/20/2023).

[18] F. Curti, B. Daino, G. D. Marchis, and F. Matera, "Statistical treatment of the evolution of the principal states of polarization in single-mode fibers", *Journal of Lightwave Technology,*, vol. 8, no. 8, pp. 1162–1166, 1990. DOI: 10.1109/50.57836.

[19] D. Fratta, "Overview and preliminary results from the porotomo project at brady hot springs, nevada: Poroelastic tomography by adjoint inverse modeling of data from seismology, geodesy, and hydrology", in *Proceedings of 42nd Workshop on Geothermal Reservoir Engineering*, Stanford, California, United States, 2017, SGP-TR–212.

[20] S. Pellegrini, G. Rizzelli, M. Barla, and R. Gaudino, "Algorithm optimization for rockfalls alarm system based on fiber polarization sensing", *IEEE Photonics Journal,*, vol. 15, no. 7100709, pp. 1–9, 2023. DOI: 10.1109/JPHOT.2023.3281670.

[21] INGV. "Italian National Institute of Geophysics and Volcanology". (2024), [Online]. Available: http://ismd.mi.ingv.it/ismd.php?tipo=lista (visited on 04/20/2024).

[22] H. Li and T. Qiu, "Continuous manufacturing process sequential prediction using temporal convolutional network", *Computer Aided Chemical Engineering*, vol. 49, pp. 1789–1794, 2022. DOI: 10.1016/B978-0-323-85159-6.50298-0.

[23] S. Hochreiter and J. Schmidhuber, "Long short-term memory", *Neural Computation*, vol. 9, no. 8, pp. 1735–1780, 1997. DOI: 10.1162/neco.1997.9.8.1735.

[24] R. B. Herrmann, L. Malagnini, and I. Munafo, "Regional moment tensors of the 2009 l'aquila earthquake sequence", *Bulletin of the Seismological Society of America*, vol. 101, no. 3, pp. 975–993, 2011. DOI: 10.1785/0120100184.